

**A Parameter Estimation Scheme for Multiscale
Kalman Smoother (MKS) Algorithm Used in
Precipitation Data Fusion**

Shugong Wang^{1,2} and Xu Liang³

Shugong Wang, Code 617, NASA Goddard Space Flight Center, 8800 Greenbelt Rd, Greenbelt,
MD 20771, USA (shugong.wang@nasa.gov)

Xu Liang, Department of Civil and Environmental Engineering, University of Pittsburgh,
Pittsburgh, PA 15261, USA (xuliang@pitt.edu)

¹Science Applications International
Corporation, McLean, Virginia, USA.

²Hydrological Sciences Laboratory, NASA
Goddard Space Flight Center, Greenbelt,
Maryland, USA.

³Department of Civil and Environmental
Engineering, University of Pittsburgh,
Pittsburgh, Pennsylvania, USA.

Abstract. A new approach is presented in this paper to effectively obtain parameter estimations for the Multiscale Kalman Smoother algorithm. This approach has demonstrated promising potentials in deriving better data products based on data of different spatial scales and precisions. Our new approach employs a multi-objective parameter estimation scheme (called MO scheme), rather than using the conventional maximum likelihood scheme (called ML scheme), to estimate the MKS parameters. Unlike the ML scheme, the MO scheme is not simply built on strict statistical assumptions related to prediction errors and observation errors, rather, it directly associates the fused data of multiple scales with multiple objective functions in searching best parameter estimations for MKS through optimization. In the MO scheme, objective functions are defined to facilitate consistency among the fused data at multiscales and the input data at their original scales in terms of spatial patterns and magnitudes. The new approach is evaluated through a Monte Carlo experiment and a series of comparison analyses using synthetic precipitation data. Our results show that the MKS fused precipitation performs better using the MO scheme than that using the ML scheme. Particularly, improvements are significant compared to that using the ML scheme for the fused precipitation associated with fine spatial resolutions. This is mainly due to having more criteria and constraints involved in the MO scheme than those included in the ML scheme. The weakness of the original ML scheme that blindly puts more weights onto the data associated with finer resolutions is overcome in our new approach.

1. Introduction

Most of weather-driven environmental simulations require reliable precipitation data as input, which significantly affects terrestrial water and energy budget, land-atmosphere interactions, ecological processes and some bio-geochemical processes. The quality of precipitation data has direct and essential impacts on the reliability and applicability of simulation results. However, none of the precipitation data are perfect enough to completely satisfy the expectations of environmental simulations, which is mainly due to the limits associated with precipitation measurements, typically including rain gauges, weather radars and weather satellites. Rain gauges are reliable at local points but poor at capturing spatial pattern of the precipitation. On the contrary, weather radars are good at capturing spatial patterns but poor at absolute magnitudes. In addition, weather radars are also limited at spatial coverage and do not work well in mountainous regions. Weather satellites further include polar orbit satellites with microwave imagers and geostationary orbit satellites with infrared imagers. Comparing these two types of satellites, the former measures precipitation at higher spatial resolutions but lower temporal resolutions while the latter is associated with coarser spatial resolutions but finer temporal resolutions. In addition to the representability of measurement instruments, uncertainty is another issue of the precipitation data, even for those produced with cutting-edge technologies, such as satellite-borne sensors [Tian and Peters-Lidard, 2010]. In order to improve the environmental simulations, it is fundamentally important to derive precipitation data products with better representability and lower uncertainty through data fusion in which

multiple precipitation measurements, even simulated precipitation by numerical weather models, are effectively combined.

Fusion of the precipitation data is generally associated with multiscales due to two reasons: (1) sensors available for precipitation measurements are associated with multiple spatial resolutions; and (2) data processing algorithms and weather/climate models are usually operated at a different scale as well. Also, environmental applications may require precipitation data at yet another different spatial resolution. Thus, data fusion algorithms for precipitation should be able to deal with input and output data at multiple scales. Furthermore, fusion of the data from different sources with different scales makes it possible to extract useful information of different sources and then have the information effectively combined to form a new dataset at the same or different spatial resolutions for applications. This is especially beneficial for hydrological and land surface simulations. As is known, precipitation data products may be good at either spatial patterns or magnitudes but hardly at both [Jayakrishnan *et al.*, 2004; Voisin *et al.*, 2008]. For example, the precipitation data product of the National Weather Service (NWS) Next Generation Weather Radar (NEXRAD) Multisensor Precipitation Estimation (MPE) has a finer spatial resolution of 4 km, which is favorable in describing spatial patterns of the precipitation. However, it is noisy and sometimes has large biases in terms of its magnitude compared to the rain gauge measurements [Wang *et al.*, 2008; Nan *et al.*, 2010]. Precipitation data products of North American Land Data Assimilation System (NLDAS) are better at describing magnitude since they are determined based on Climate Prediction Center (CPC) daily gauged precipitation data [Cosgrove *et al.*, 2003]. Nevertheless, they are not very good at describing the spatial patterns due to their relatively coarse spa-

tial resolution, i.e., 0.125° . It is reasonable to infer that more reliable precipitation data products can be derived by combining the NEXRAD MPE data with the NLDAS data through a multiscale data fusion approach [Nan *et al.*, 2010]. Moreover, if precipitation data products at multiple spatial resolutions are required, the advantages of employing a multiscale precipitation fusion approach becomes even more obvious.

Among the data fusion algorithms such as artificial neural network [Sorooshian *et al.*, 2000], Kalman Filter [Smith and Krajewski, 1991; Ushio *et al.*, 2009] and statistical methods [Ly *et al.*, 2011], the Multiscale Kalman Smoother (MKS) algorithm [Chou and Willsky, 1991; Chou *et al.*, 1994; Willsky, 2002; Parada and Liang, 2004] offers many good features which are particularly important for conducting the multiscale precipitation data fusion as illustrated in Wang *et al.* [Wang *et al.*, 2011] through a systematic investigation and analyses. The MKS algorithm is based on the theory of Markov random field over space. It can easily fuse multi-resolution (multiscale) data organized by a quadtree, as shown in Figure 1. With this MKS algorithm, fused precipitation at any scale represented by the quadtree can be derived. The MKS algorithm, also bearing the name of scale-recursive estimation (SRE) method, has been examined in multiscale precipitation data fusion applications and demonstrated great potentials. For example, Gorenburg *et al.* [2001] evaluated the SRE method in the assimilation of radar precipitation data and satellite precipitation data, which are at 2.5 km and 15 km respectively. The SRE method exhibited descent capability by reproducing withheld radar measurements with fused precipitation data. Such kind of evaluation has also been done by Van de Vyver and Roulin [2009] with precipitation data of weather radar and satellite microwave measurements. Similarly, Bocchiola [2007] examined SRM method upon fusing precipitation

measurements of TMI radiometer and PR radar boarded on the TRMM satellite and NEXRAD radar. In addition to studies in the spatial domain, SRE method has also been evaluated in the time domain to fuse precipitation data at varying temporal resolutions [Tustison *et al.*, 2002]. In addition to the applications to the precipitation data fusion, the MKS algorithm has also been applied to soil moisture data assimilation [Parada and Liang, 2004, 2008; Kumar, 1999], altimetry data fusion [Slatton *et al.*, 2001, 2002] and imagery data fusion [Huang *et al.*, 2002; Simone *et al.*]. All of these studies have shown that more reliable data products can be derived with the MKS algorithm by fusing or assimilating multiscale data if the algorithm parameters are determined properly.

MKS is an algorithm with high degree of freedom due to its relatively large number of parameters, which are involved in characterizing measurement errors, prediction errors and state-space equations. Performance of the MKS algorithm, like other algorithms, heavily depends on the proper estimations of these parameters. The Maximum Likelihood (ML) based methods are typically used in the parameter estimation of the MKS algorithm because of its simple statistical formulation and high computational efficiency [Chou, 1996; Digalakis *et al.*, 1993; Bocchiola, 2007]. Applying the Expectation-Maximization (EM) method, the maximum likelihood parameters of the MKS algorithm can be determined through iterations when there are latent variables involved in the MKS model framework e.g., [Kannan *et al.*, 2000; Parada and Liang, 2004; Gupta *et al.*, 2006]. However, it is quite often that both the ML method and the EM method only find local optimums but not global optimal estimations of the MKS parameters in practical applications. This is mainly because that the ML and EM methods strictly assume measurement errors and prediction errors to be independent and to follow zero-mean Gaussian distributions. Such

assumptions make the derivation of the likelihood functions straightforward and simple to implement, but they are too strong to be generally satisfied by the precipitation data. Therefore, the MKS algorithm cannot have the precipitation data optimally fused at all spatial scales when the ML method and the EM method are applied, as illustrated and discussed in [Wang *et al.*, 2011]. In fact, [Wang *et al.*, 2011] showed that the fused precipitation data was significantly improved at the coarse resolution (e.g. $1/8^\circ$) while the improvement at the fine resolution (e.g. $1/32^\circ$) is limited or even deteriorated if the finer resolution data are much noisier than the coarse resolution data. This is due to a combined effect that only local optimal parameters are found and that too much weight is placed to the finer resolution precipitation data by the EM method associated with the MKS algorithm, which is fine if the noisy levels at the different scales are comparable. In this study, we present a new scheme to improve the parameter estimations for the MKS algorithm so that the weaknesses of the ML method are overcome or at least mitigated while the strengths of the ML method are kept and that the improvements are achieved at multiple scales (i.e., at both coarse and fine scales).

The new parameter estimation scheme for the MKS algorithm is primarily designed to improve the performance of the MKS algorithm at finer resolutions in the multiscale data fusion applications. The new scheme is based on a multi-objective optimization approach, and is referred to as MO scheme hereafter. Similarly, we refer the EM method that is used to estimate the maximum likelihood parameters of the MKS algorithm to as ML scheme hereafter. Different from maximizing only a log-likelihood function in the ML schemes, the MO scheme maximizes a number of objective functions, which are metrics directly related to the objectives of the multiscale precipitation data fusion.

To solve the multi-objective optimization problem investigated in this study, we use a multi-objective particle swarm optimization (MOPSO) algorithm. The particle swarm optimization (PSO) algorithm was firstly proposed by *Kennedy and Eberhart* [1995], and it has been proved to be effective and efficient for optimizing hydrological parameters [Gill *et al.*, 2006]. In addition, the MOPSO algorithm has been shown to be effective for different multi-objective optimization problems [Hu and Eberhart, 2002; Hu *et al.*, 2003]. In this study, we have designed and implemented a parallel MOPSO algorithm to solve our multi-objective optimization problem.

In the remaining part of this paper, a briefly description of the MKS algorithm and the EM scheme is provided in section 2 to have this paper self-contained. Detailed description and formulation of the MO scheme are presented in section 3. Evaluations of the MO scheme are presented in section 4 through a Monte Carlo experiment and 12 comparison experiments. A summary of this study is included in section 5.

2. Descriptions of the MKS algorithm and the ML Scheme

2.1. The MKS Algorithm

In the application of the MKS algorithm to precipitation data fusion, scale means the spatial resolution of precipitation data. The MKS algorithm includes a fine-to-coarse sweep of the Kalman filtering step and a coarse-to-fine sweep of the Kalman smoothing step. Both sweeps are conducted along a multiscale tree, as shown in Figure 1. In the scale domain, a linear state-space model that relates measurements at neighboring resolutions is given as follows:

$$X(t) = A(t)X(t\bar{\gamma}) + w(t) \quad (1)$$

$$P(t) = A^2(t)P(t\bar{\gamma}) + Q(t) \quad (2)$$

where $X(t)$ and $X(t\bar{\gamma})$ represent the precipitation estimates at a child node and its parent node, respectively, $w(t)$ is the prediction error following $N(0, Q(t))$, $Q(t)$ is the variance of $w(t)$, $P(t)$ and $P(t\bar{\gamma})$ are the error variances of $X(t)$ and $X(t\bar{\gamma})$, and $A(t)$ is a transition operator mapping precipitation amount from a parent node to a child node.

Given the prior estimates of the precipitation amount at the root node and its associated error variance, which are denoted with $X(0)$ and $\Sigma(0)$ respectively, the unconditional estimates of precipitation and their error variances at the remaining nodes of the multiscale tree can be computed using equation (1) and (2). Such a step is referred as initialization. After that, an upward sweep is conducted from the leaf nodes toward the root node with the inverted forms of equations (1) and (2) and a measurement equation

$$Y(t) = C(t)X(t) + v(t) \quad (3)$$

where $Y(t)$ is the measurement at node t , $C(t)$ is a transition operator mapping precipitation amount to measurement, $v(t)$ is the variance of measurement error following $N(0, R(t))$. This step indeed is Kalman filtering at the scale domain. Once it is done, all unconditional estimates of precipitation have been updated according to measurements at their and finer resolutions. Following the upward sweep, a downward sweep is conducted from the root node toward the leaf nodes to refine precipitation estimates according to measurements at coarser resolutions through Kalman smoothing. For a complete formulation of the MKS algorithm for general purposes, readers are referred to *Kannan et al.* [2000]; *Parada and Liang* [2004].

In a simple case that measurements are available at all nodes of a multiscale tree (denoted with \mathcal{T}), the MKS algorithm has a set of parameters, including $\Sigma(0)$ and $\{A(t), C(t), Q(t), R(t) | t \in \mathcal{T}\}$. Since all measurements have been converted into precipitation amounts, we can set $A(t) = 1.0$ and $C(t) = 1.0$ for all nodes in precipitation data fusion. However, the rest of the parameters, namely $\Sigma(0)$, $R(t)$ and $Q(t)$ need to be estimated. In reality, $R(t)$ and $Q(t)$ may vary over space even for measurements at the same scale. If $R(t)$ and $Q(t)$ are to be estimated at every node, the number of parameters would be more than the number of measurements, i.e., the number of nodes with valid measurements. In this instance, the parameters would be hard to be estimated adequately. In order to resolve this issue, we assume that $R(t)$ and $Q(t)$ are scale homogeneous. In other words, they are respectively identical for measurements at the same scale. Consequently, the number of parameters is significantly reduced to be much smaller than the number of measurements. Therefore, the parameters can be estimated based on available measurements without any further assumptions or constraints.

2.2. The ML Scheme

Assuming that the relationships described by equation (1) and (2) are independently held at all nodes of a multiscale tree (\mathcal{T}), the log-likelihood function can be expressed as follows, where we denote the parameter set of the MKS algorithm as θ ($\theta = \{\Sigma(0), R(t), Q(t) | t \in \mathcal{T}\}$)

$$\begin{aligned} \mathcal{L}(X, Y | \theta) = & -\frac{1}{2} \sum_{t \in \mathcal{T}_c} \{ \log(Q(t)) + [X(t) - A(t)X(t\bar{\gamma})]^2 Q(t)^{-1} \} \\ & -\frac{1}{2} \sum_{t \in \mathcal{T}_m} \{ \log(R(t)) + [Y(t) - C(t)X(t)]^2 R(t)^{-1} \} \end{aligned} \quad (4)$$

where \mathcal{T}_c represents a subset of \mathcal{T} except the root node, \mathcal{T}_m represents a subset of \mathcal{T} with measurements, and Y represent measurements. Given measurements Y , precipitation estimates X are dependents of the parameter set θ . Therefore, $\mathcal{L}(X, Y|\theta)$ can be regarded as a function of θ with given measurements and accordingly θ can be estimated by maximizing $\mathcal{L}(X, Y|\theta)$.

In the ML scheme, parameter set θ is determined using the EM algorithm, which includes an expectation step (E-step) and a maximization step (M-step). In the multiscale precipitation data fusion applications, one cycle of the upward sweep and the downward sweep of the MKS algorithm serves as the E-step, which computes smoothed estimates of precipitation as statistical expectation. After the E-step, parameters θ are the only free variables in $\mathcal{L}(X, Y|\theta)$. The M-step is to maximize the log-likelihood (Equation 4) by adjusting the parameters using a numerical approach, such as gradient-based methods. Details about the ML scheme with the EM algorithm can be found in *Kannan et al.* [2000].

3. Multi-Objective Parameter Scheme

Our multi-objective (MO) scheme for the MKS algorithm is explicitly constructed on the expectation of multiscale precipitation data fusion. Generally, multiscale precipitation data fusion is to derive new precipitation products, which are expected to be better in representing the spatial patterns and magnitudes of the precipitation at the original scales of the input data or at any other scales depending on applications. But, on the other hand, these fused datasets should also be expected to inherit, more or less, the characteristics of the spatial patterns and the magnitudes of their original data sources. In principle, if the parameters of the MKS algorithm are reasonably estimated for representing the errors

associated with each data source, then the spatial patterns and the magnitudes of the fused precipitation data derived with MKS algorithm should be consistent with each other at all output scales according to the quality of each of the data sources. However, due to the limitations discussed in section 1, neither the popular maximum likelihood method nor the EM method is adequately effective in finding the MKS parameters in all practical applications due to the local maximums, which usually over-weight the observations at finer resolutions. Our idea is thus to force the optimization search to find a better optional parameter set by introducing more physically sound constraints. To this end, we introduce two spatial correlation related objective functions to constrain the search for a typical case of fusing two data sources. In order to avoid over smoothing, we also introduce some other objective functions to maximize maximum precipitation or maximum information in fused precipitation data.

In a multiscale precipitation data fusion, the consistency in spatial patterns among output scales can be measured either with correlation (Corr) or root mean square error (RMSE). The former focuses more on spatial patterns while the latter focuses more on magnitudes. Correlation has intuitive statistical meaning and fixed lower and upper boundaries, i.e., -1.0 and 1.0. In addition, correlation is monotonically related to RMSE in the multiscale precipitation data fusion using the MKS algorithm. That is, for the same data, RMSE decreases with an increase in Corr. Therefore, correlation would be a proper measure of the consistency among fused precipitation data.

In order to calculate the correlation of two datasets associated with two different spatial scales (e.g., $1/8^\circ$, and $1/32^\circ$), one can either aggregate the finer resolution data of $1/32^\circ$ into the coarser resolution (i.e., $1/8^\circ$) or disaggregate the coarser resolution data of $1/8^\circ$

into the finer resolution (i.e., $1/32^\circ$). Subsequently, one can calculate the correlations at both of these resolutions. For the purpose of this study, we try to obtain the correlation between the two fused precipitation data at $1/8^\circ$ as high as possible. For example, a value of 1.0 indicates that the finer fused precipitation data (e.g., $1/32^\circ$) has a perfect consistency with the fused precipitation data at the coarser resolution (e.g., $1/8^\circ$). While for the correlation at $1/32^\circ$, we try to have the correlation between the two fused precipitation data close to a target correlation value, which is close but less than 1.0. For example, the target correlation can be 0.90. This roughly implies that 90% spatial pattern of the fused precipitation data at the finer resolution is consistent with the fused precipitation data at the coarser resolution while the 10% differences are due to the variations associated with the details of the fused data at the finer resolution compared to the fused data at the coarser resolution. In this way, one can basically use the correlation measure to facilitate the consistency among the fused precipitation datasets at two different spatial scales, i.e., at both the finer and coarser resolutions.

The MKS algorithm is a smoother by nature. If parameters are not well estimated, there is a risk that the fused precipitation data are over smoothed. Once the over-smoothing happens, the maximum value of the fused precipitation would be significantly smaller than that without being over-smoothed. Mean while, the information content of precipitation data will be partially lost. Thus it is important to avoid such over-smoothing from happening. Two approaches are proposed independently with the MO scheme. One approach is to maximize the largest values of fused precipitation data at all of output scales. The other is to maximize the Shannon information entropy of fused precipitation data at all

output scales. The advantages and disadvantages of these two approaches is going to be illustrated in section 4.

Based on the discussions above, we propose to improve the estimation of the MKS parameters by formulating a multi-objective optimization problem, in which we introduce two groups of objective functions. The first group include a number of spatial correlations as measures of consistency among fused precipitation data at output scales. The second group include a number of maximization functions of either largest value or the information entropy of fused precipitation data at output scales. In the following, specific objective functions are given for a simple case with two precipitation data sources. For notational convenience, let us specify X to represent the fused precipitation data, superscript $-$ and $+$ to represent, respectively, before and after the data fusion, subscript c and f to represent, respectively, a coarse and a fine resolution, $c \rightarrow f$ to represent disaggregation from a coarse resolution to a fine resolution and $f \rightarrow c$ to represent aggregation from a fine resolution to a coarse resolution. The estimation of the MKS parameters can be achieved via maximizing the following four objective functions if maximization of largest value of fused precipitation data is used to avoid over-smoothing:

$$g_1(\theta) = Corr(X_c^+, X_{f \rightarrow c}^+) \quad (5)$$

$$g_2(\theta) = -|Corr(X_f^+, X_{c \rightarrow f}^+) - \rho| \quad (6)$$

$$g_3(\theta) = \max(X_c^+) \quad (7)$$

$$g_4(\theta) = \max(X_f^+) \quad (8)$$

in which, $g_1(\theta)$ measures the consistency of the fused precipitation data at a coarse resolution; $g_2(\theta)$ measures the consistency of the fused precipitation data at a fine resolution,

ρ is a slack parameter to relax the consistency requirement at the finer resolution; $g_3(\theta)$ and $g_4(\theta)$ are the maximum values of the fused precipitation data at the coarse and the fine resolutions, respectively. As mentioned previously, the slack parameter is added to avoid over-smoothing at the finer resolution. If maximization of information entropy is used to avoid over-smoothing, $g_3(\theta)$ and $g_4(\theta)$ will be replaced with $g_5(\theta)$ and $g_6(\theta)$ as shown in the following:

$$g_5(\theta) = - \sum_{i=1}^n p(x_{c,i}^+) \log p(x_{c,i}^+) \quad (9)$$

$$g_6(\theta) = - \sum_{i=1}^n p(x_{f,i}^+) \log p(x_{f,i}^+) \quad (10)$$

where n is number of precipitation bins and i is the index of precipitation bin. In this study, precipitation values are evenly categorized into bins with a bin size of 0.1 mm.

The multi-objective optimization problem formulated with equations (5), (6), (7) and (8) (or (9) and (10)) can be solved in many ways. In this study (i.e., MO scheme), it is solved with a multi-objective particle swarm optimization (MOPSO) algorithm [Wang, 2011]. Similar to most multi-objective optimization algorithms, the MOPSO algorithm returns not a single optimal solution but a set of Pareto frontiers. However, only one optimal parameter set is to be used in the precipitation data fusion using the MKS algorithm. Our strategy of selecting the optimal solution from the Pareto frontiers includes two steps: (1) select solutions with the largest $g_1(\theta) + g_2(\theta)$, and (2) find the solution with the largest $g_3(\theta) + g_4(\theta)$ or $g_5(\theta) + g_6(\theta)$ from those identified in step (1). Note that the solution of our proposed MO scheme can be obtained by any handy multi-objective optimization solver, such as genetic algorithms and simulated annealing algorithms.

We hypothesize that by applying the MO scheme to the four objective functions described by equations (5), (6), (7) and (8), we can not only obtain better MKS parameter

estimates, but also these estimates are able to keep the essential strengths of those associated with the ML scheme and overcome, at least to a large extent, the weaknesses of the ML scheme. This hypothesis will be assessed by adding the likelihood function, i.e. Equation (4), as one more objective function in section 4.

4. Evaluations

4.1. Experiment Design

Two types of experiments are designed to evaluate the ML scheme and our proposed MO approach. The first is a Monte Carlo experiment, which demonstrates the limitation of the ML scheme and illustrates the rationality for developing the MO scheme. The second is a comparison experiment, which include between-group comparisons and in-group comparisons. The effectiveness of the ML scheme and the MO scheme is statistically evaluated through between-group comparisons. The two approaches of avoiding over-smoothing are evaluated through in-group comparisons.

To make the analysis of this study be more representative, in other words, closer to real applications, we select a large study domain (Figure 2), bounded by longitudes (88°W , 84°W) and latitudes (37.75°N , 41.75°N), for both types of experiments. The domain includes 128×128 grids at $1/32^{\circ}$ resolution and 32×32 grids at $1/8^{\circ}$ resolution. The average annual precipitation in this area is about 1,000 mm. Precipitation is relatively evenly distributed throughout a year. Typically, precipitation is steady and of long duration in winter and early spring and short but of high intensity during late spring and summer.

Synthetic noisy precipitation data are used in both types of experiments to evaluate the effectiveness of our new approach (i.e., the MO scheme), compared to the ML scheme, in

obtaining the MKS parameter estimates. The synthetic noisy data are generated based on a set of hourly NEXRAD MPE precipitation data and noises added to the MPE data. The MPE data, which were at a spatial resolution of 4 km and in a specific data format, namely XMRG, were projected into the longitude-latitude coordinate system and re-sampled into $1/32^\circ$ and $1/8^\circ$ resolutions, respectively. The noises are generated based on the Gaussian distributions with zero mean and different standard deviations that are prescribed according to the MPE data.

These standard deviations are set to be proportional to the standard deviations of the MPE data. For example, at hour k one has the MPE precipitation data (i.e., true data) X_k of a 2-dimensional (2-D) field. Based on it one can calculate the standard deviation of X_k , denoted as s_k . Then, white noises can be sampled from the Gaussian distributions of $\mathcal{N}(0, n_i s_k)$, where n_i , called noise level hereafter, is a multiple of s_k that controls the level of perturbation. The sampled values (i.e., the noises) from $\mathcal{N}(0, n_i s_k)$ are then added to X_k to obtain the synthetically generated noisy precipitation datasets that correspond to different noisy levels. If $n_i = 1$, the standard deviation of added noises is actually the same as the standard deviation of the real MPE precipitation data of the k^{th} hour. Note that the synthetically generated precipitation value may be negative if the generated white noise has a large negative value. In such a situation, a new value of the white noise will be generated until the synthetic precipitation value is not negative. In other words, the noises generated are from truncated Gaussian distributions.

This adaptive approach brings three favorable features to the synthetic precipitation datasets. First, the magnitudes of generated data are guaranteed to be non-negative, which is essential to describe precipitation. Second, the added noises are generated based

on normal distribution but not strictly normally distributed due to the noise re-generation procedure. Third, it is easy to control the magnitudes of the noises by adjusting the noise level, i.e. n_i .

For details of this synthetic data generation method and the properties of its generated precipitation data, readers are referred to the work by Wang et al. [2011]. We use synthetic precipitation datasets here to evaluate the MO and ML schemes. It is mainly due to the advantage of being able to control the magnitudes of errors/noises to be included in the generated precipitation datasets. Thus, using such datasets would be more effective in evaluating the strengths and weaknesses of the MO and ML schemes on the MKS parameter estimates and the impacts of the MO and ML schemes on precipitation data fusion results using the MKS algorithm. In fact, the approach of using synthetic data has been widely used in data assimilation study for the convenience of performance evaluation [e.g., Walker and Houser, 2004].

In both types of experiments, we apply the MKS algorithm to fuse one set of precipitation data at a coarser resolution, i.e. $1/8^\circ$ with the other set of precipitation data at a finer resolution, i.e. $1/32^\circ$. Based on the NEXRAD MPE precipitation data, we have two sets of the synthetic precipitation data generated for an entire year of 2003 at both the coarser ($1/8^\circ$) and the finer ($1/32^\circ$) resolutions. There are totally 2246 precipitation events in each set of the synthetic data. As mentioned in section 2, we need to organize the input data in a multiscale tree, which is illustrated in Figure 1 with an example, before applying the multiscale data fusion using the MKS algorithm. The total number of the scales of such a multiscale tree depends on the size of an experiment domain and the resolutions of the input data. In this study, the multiscale tree built for the experiment

domain has 8 scales indexing from 0 to 7. Resolutions of $1/8^\circ$ and $1/32^\circ$ correspond to, respectively, scales 5 and 7 of the multiscale tree. Therefore, we also call the data at $1/8^\circ$ and $1/32^\circ$ resolutions as scale 5 data and scale 7 data, respectively

In this study, three series of synthetic precipitation datasets at scale 5 are generated with the noise levels of $n_5=1.0, 2.0$ and 3.0 and four series of synthetic precipitation datasets at scale 7 are generated with the noise levels of $n_7=1.0, 2.0, 3.0$ and 4.0 . Each data series includes 2246 synthetic hourly precipitation fields over the experiment domain. There is one more noise level employed at scale 7 to describe the reality that precipitation data at finer resolutions may be noisier than those at coarser resolutions.

The goal of the multiscale precipitation data fusion is to improve the spatial pattern and the magnitude of precipitation data at multiple scales. To evaluate whether such a goal is achieved, we use $\Delta Corr_s = Corr(X_s^{true}, X_s^+) - Corr(X_s^{true}, X_s^-)$ and $\Delta RMSE_s = RMSE(X_s^{true}, X_s^-) - RMSE(X_s^{true}, X_s^+)$ as the metrics at scale s , where X_s^{true} represents the true precipitation amounts, X_s^- represents the synthetically generated precipitation values, and X_s^+ represents the fused precipitation values. $Corr(X_s^{true}, X_s^-)$ and $Corr(X_s^{true}, X_s^+)$ are also expressed as $Corr_s^-$ and $Corr_s^+$ for short. Similarly, $RMSE(X_s^{true}, X_s^-)$ and $RMSE(X_s^{true}, X_s^+)$ are expressed as $RMSE_s^-$ and $RMSE_s^+$ for short as well. The effectiveness of the ML and MO schemes is evaluated using $\Delta Corr$ and $\Delta RMSE$. If a parameter estimation scheme helps to result in a larger $\Delta Corr$, it means that this scheme is better than the other schemes for improving the spatial pattern of the precipitation data. Similarly, if a parameter scheme helps to result in a larger $\Delta RMSE$, it means this scheme is better than the other scheme for improving the magnitudes of precipitation data.

For clear discussions we use box plots to illustrate most of experiment results conducted in this study. Box plots are a convenient way of graphically depicting distributions of samples with the lower (25^{th}) quartile, median, the upper (75^{th}) quartile, 1.5 IQR (interquartile range) of the lower quartile, and 1.5 IQR of the upper quartile. If the samples approximately follow a normal distribution, over 99% of them would fall within the upper and the lower whiskers shown between the 1.5 IQRs of the lower quartile and the upper quartile. In addition, box plots also mark the mean values of each statistical variable, which are used in the result analysis for the comparison experiments in section 4.3. Figure 3 shows the box plots for correlation (vertical axes in the two upper plots) and RMSE (vertical axes in the two lower plots) which are obtained between the 2246 true and synthetic precipitation fields of 2003. The horizontal axes represent the values taken for n_5 and n_7 , respectively. From Figure 3, one can see, as expected, that the correlation (RMSE) decreases (increases) as the variance increases for both scales 5 and 7, respectively. Figure 3 provides a benchmark for this study as both the MO scheme and the ML scheme are expected to generate higher *Corr* and lower *RMSE* at scale 5 and scale 7 than the corresponding ones shown in Figure 3.

4.2. Monte Carlo Experiment

Monte Carlo experiments are designed to examine the effectiveness of the ML scheme in the multiscale precipitation data fusion process using the MKS algorithm. Based on the results of the Monte Carlo experiment, one can see the weaknesses of the ideal/theoretical ML scheme when it is applied to real-world applications, in which assumptions and conditions required by the ML scheme and the MKS algorithm are not met exactly. Through

the Monte Carlo experiment results, one can also see the rationale behind in developing the MO scheme for the MKS algorithm.

The Monte Carlo experiment includes three steps: (1) generating a large amount of parameter sets in their feasible spaces, (2) conducting data fusion with generated parameter sets, and (3) computing the corresponding log-likelihood, $Corr_s^+$ and $RMSE_s^+$. As described in section 2.2, the ML scheme identifies parameters for the MKS algorithm by maximizing the log-likelihood function (i.e., equation 4). If all the requirements/ conditions are met, the ML scheme can find the global optimal parameter estimations for the MKS algorithm used in multiscale precipitation data fusion. Thus, $Corr_s^+$ ($s=5$ and 7) should reach its maximum and $RMSE_s^+$ should reach its minimum when the log-likelihood reaches its maximum.

In this study, only one representative precipitation event is selected for conducting the Monte Carlo experiment. Occurred at 09Z 09/22/2003, the precipitation event was a summer storm and covered about 95% area of the experiment domain shown in Figure 2. In the Monte Carlo experiment, the noise levels, i.e. n_5 and n_7 , are set to 2.0 when generating the synthetic precipitation data at both scales 5 and 7. We randomly sample 1,000,000 parameter sets, including $\Sigma(0)$, $Q(s)$ ($s=1, 2, \dots, 7$), and $R(s)$ ($s=5$ and 7) using a uniform distribution. Since all parameters are essentially error variances of precipitation data, the feasible range is set to $[0.1, 10.0]$ for each of them. After fusing the precipitation data at scales 5 and 7 with all sampled parameters using the MKS algorithm, we compute the log-likelihood, $Corr_5^+$, $Corr_7^+$, $RMSE_5^-$ and $RMSE_7^+$ corresponding to every parameter set.

The effectiveness of the ML scheme is examined based on the relationships between the log-likelihood and $Corr_5^+$, $Corr_7^+$, $RMSE_5^+$, $RMSE_7^+$ respectively, which are shown in the scatter plots of Figure 4. An essential finding from Figure 4 is that the ML scheme has different effectiveness at scale 5 and scale 7. First, it is much more effective at scale 5 than at scale 7. Both $Corr_5^+$ and $RMSE_5^+$ converge to their maximum and minimum values, respectively, when the log-likelihood approaches its maximum. As an objective function, the log-likelihood defined in equation 4 appears to be consistent to the correlation and RMSE at the coarser resolution in the Monte Carlo experiment. This provides an adequate proof that the ML scheme is more likely to be able to produce parameter estimates for the MKS algorithm that are in favor of the fused precipitation data products at coarser resolutions.

On the other hand, the ML scheme is not guaranteed to result in parameter estimates which are also effective for the fused data at scale 7. That is, local optimals rather than global optimals are likely obtained by the ML scheme in this case when the requirements and conditions of the ML scheme are fully met. As shown in Figure 4, $Corr_7^+$ may converge to two substantially different extreme values when the log-likelihood approaches to its maximum. One extreme value is closed to the upper bound of $Corr_7^+$ while the other is closed to the lower bound of $Corr_7^+$ (see Figure 4). Similar situation also occurs to $RMSE$ as shown in Figure 4. If $Corr_7^+$ goes to its lower extreme value or $RMSE_7^+$ goes to its upper extreme value, there will be no gain through the precipitation data fusion in terms of improving the spatial patterns and magnitudes of the precipitation data at scale 7. This example clearly indicates that the estimated parameters using the ML scheme may not work for the fused precipitation data at finer resolutions due to the combined

effects of encountering local maximums and the required conditions for the algorithms being not fully met in the real-world applications.

Nevertheless, there are no monotonous relationships between the log-likelihood and $Corr_s^+$ or $RMSE_s^+$ for $s=5$ and 7. An increase of the log-likelihood does not necessarily mean an increase of $Corr_s^+$ or a decrease of $RMSE_s^+$. In the ML scheme used in this study, the log-likelihood is maximized using the EM algorithm, which usually stops iterating when the log-likelihood reaches a local maximum or after a given number of iterations is reached. This example clearly illustrates the limitations of the ML scheme.

Findings of the Monte Carlo experiments here are consistent with the results shown in the study by Wang *et al.* [2011], which found that the improvements at a coarser resolution are much more significant than those at a finer resolution when the precipitation datasets are fused using the MKS algorithm with the ML scheme as its parameter estimation method. The maximization of the log-likelihood is neither a necessary nor a sufficient condition for achieving improvements of the fused precipitation data at finer resolutions. If one wants to achieve improvements at multiple scales, especially at finer resolutions, there is a critical need to develop a new scheme to estimate the parameters of the MKS algorithm.

4.3. Comparison Experiments

A series of comparison experiments are designed to illustrate the strengths and limitations of the proposed MO scheme as opposed to the ML schemes. Totally 12 scenarios of multiscale precipitation data fusion have been made through combining noisy precipitation data at a finer resolution and a coarser resolution. As described in section 4.1, we have generated the synthetic noisy precipitation data of the coarser resolution (i.e. $1/8^\circ$)

with three noise levels (i.e. $n_5=1.0, 2.0$ and 3.0) and the synthetic noisy precipitation data of the finer resolution (i.e. $1/32^\circ$) with four noise levels (i.e. $n_7=1.0, 2.0, 3.0$ and 4.0). These synthetic precipitation data can form 12 (i.e., 3×4) combinations for conducting the MKS data fusion. For example, the combination of $n_5 = 2.0$ and $n_7 = 4.0$ indicates a scenario in which a set of noisy precipitation data at $1/8^\circ$ resolution is fused with much noisier data at $1/32^\circ$ resolution. In this particular example, the noisy level at the finer resolution data is about two times of that at the coarser resolution. Generally speaking, if $n_5 > n_7$, it means that the combination mimics a scenario in which the coarser resolution data are fused with less noisy finer resolution data. On the other hand, if $n_5 < n_7$, it means that the combination mimics a scenario in which the finer resolution data are fused with less noisy coarser resolution data. If $n_5 = n_7$, it means that the combination mimics a scenario in which the coarser resolution data is fused with the finer resolution data that has similar or comparable level of the noises. Since the precipitation data at finer resolutions is usually noisier than the precipitation data at coarser resolutions in real world, the maximum value of n_7 (i.e. 4.0) is thus greater than the maximum value of n_5 (i.e. 3.0).

Each of the 12 scenarios has two series of the synthetic precipitation data to be fused. The two series, at $1/32^\circ$ and $1/8^\circ$ resolutions respectively, both include 2246 noisy precipitation fields throughout year 2003 in the experiment domain. The two series of data have been fused using the MKS algorithm field by field. The ML scheme is firstly used in the parameter estimation for the MKS algorithm. Fused precipitation data with the ML scheme, notated with number 0 hereafter, are used as references to evaluate the MO schemes with three approaches to avoid over smoothing. Equations (5) and (6) are the

core part of the MO scheme. No matter which approach is used, they are part of objective functions. The first approach uses equation (7) and (8) to maximize the maximum values of fused precipitation data; the second approach uses the likelihood function (equation 4) in addition to equations (7) and (8); the third approach uses equations (9) and equations (10) to maximize the information contents of fused precipitation data at output resolutions. For notational convenience, the MO schemes with the three approaches are marked with number 1, 2, and 3 in result plots and analysis.

Even though the multiscale precipitation data fusion using the MKS algorithm can output fused precipitation datasets at any resolutions from the finest to the coarsest scale of the multiscale tree (see Figure 1), we just output the fused precipitation datasets at $1/8^\circ$ and $1/32^\circ$ resolutions for evaluating the effectiveness of the MO scheme versus the ML scheme since the true data are available at these two scales. For each scenario, we compute $\Delta Corr_s$ and $\Delta RMSE$ ($s = 5, 7$) for all of the 2246 precipitation fields (i.e., precipitation images) for schemes 0, 1, 2, and 3. We then compare the statistics (e.g., mean, quartiles) of $\Delta Corr_s$ and $\Delta RMSE_s$, instead of the $\Delta Corr_s$ and $\Delta RMSE_s$ for individual precipitation fields among schemes 0, 1, 2, and 3. That is the distributions of $\Delta Corr_s$ and $\Delta RMSE$ are compared in the following discussions. The large number of samples, i.e. 2246, included in the analyses guarantees the statistical significance of our comparison studies. Thus, the overall performances of each individual scheme (i.e., the MO and ML schemes) can be more objectively evaluated.

Figure 5 shows the box plots of $\Delta Corr_s$ ($s = 5, 7$) for the 12 scenarios. Each of them has results obtained with the ML scheme and the three MO schemes. In Figure 5, if a MO scheme leads to a larger mean of $\Delta Corr_s$, it indicates that the MO scheme statistically

perform better than the ML scheme on average based on the 2246 precipitation fields investigated. Similarly, if a MO schemes results in a larger value of median, it indicates that the MO scheme perform better than the ML scheme over half of the 2246 precipitation fields for the given combination of n_5 and n_7 . Otherwise, it indicates that the ML scheme performs better than the MO scheme.

In Figure 5, the differences of $\Delta Corr_5$ between results of the ML scheme and the MO schemes are relatively small for the 12 scenarios compared to the corresponding differences of $\Delta Corr_7$. In terms of the $\Delta Corr_5$ values, the MO schemes are better in eight scenarios, while the ML scheme is better in 4 scenarios in which the noise levels at the finer resolution are higher or much higher than those at the coarser resolution. These four scenarios are $(n_5 = 1, n_7 = 2)$, $(n_5 = 1, n_7 = 3)$, $(n_5 = 1, n_7 = 4)$, and $(n_5 = 2, n_7 = 4)$. Such results indicate that the MO schemes are slightly under performed than the ML scheme on improving the spatial pattern of the coarser precipitation data when the coarser precipitation data have better or much better quality than the finer precipitation data. For the results of scenarios in which $n_5 \geq n_7$, the MO schemes produce larger values of the mean and the median of $\Delta Corr_5$ than those of the ML scheme. This indicates that the MO schemes perform better than the ML scheme in terms of improving the spatial patterns of the precipitation data at coarser resolution when the precipitation data at the coarser resolution have poorer quality than those at the finer resolution. In addition, the box plots in Figure 5 reveals that the improvements with the MO schemes are greater than those with the ML scheme when the coarser precipitation data have much poorer quality than the finer precipitation data.

In Figure 5, it can be found that the three MO schemes perform closely in terms of improving $\Delta Corr_5$. For most of the scenarios, the #2 MO scheme is slightly better than the #1 MO scheme and the #3 MO scheme is slightly better than the #2 MO scheme in terms of the mean, the median, the upper quartile and the lower quartile. However, the differences are very small. Comparing to the #1 MO scheme, the computational time of the #2 MO scheme is almost doubled because the log-likelihood function is added as an extra objective function. The gain of the #2 MO scheme over the #1 MO scheme is almost negligible. This implies that the 4 objective functions of the #1 MO scheme include most of the information which could be introduced by the log-likelihood function (i.e., Eq. 4) for the purpose of improving precipitation data at a coarser resolution. The #3 MO scheme also takes about double the computation time of the #1 MO scheme, because computing information entropy of equations 9 and 10 takes much longer time than finding the maximum precipitation values (equations 7 and 8). Even though the gain of the #3 MO scheme is also minor at the coarser resolution compared to the #1 MO scheme, but the gain at the finer resolution is more noticeable as can be seen in Figure 5.

For the fused precipitation at the finer resolution, i.e., $1/32^\circ$ (scale 7), Figure 5 shows that the MO schemes perform better or much better than the ML scheme on improving the spatial patterns of the fused precipitation at this resolution for all of the 12 scenarios. It does not matter which data quality situations are at the coarser finer resolutions, i.e. either $n_5 > n_7$, $n_5 = n_7$ or $n_5 < n_7$, the mean, the lower and upper quartiles, the median, and the two whiskers of $\Delta Corr_7$ of the three MO schemes are always significantly higher than those of the ML scheme. Specifically, all lower quartiles of $\Delta Corr_7$ of the three ML

schemes are larger than the upper whiskers of corresponding $\Delta Corr_7$ of the ML scheme when $n_5 \geq n_7$. This indicates that the MO schemes performs better than the ML scheme for at least 75% of the 2246 precipitation fields. When $n_5 < n_7$, all of the lower whiskers of $\Delta Corr_7$ of the MO schemes are larger than the lower whiskers of corresponding $\Delta Corr_7$ of the ML scheme, which indicates that the MO schemes performs better than the ML scheme for at least 90% of the 2246 precipitation fields. This superiority of the MO schemes over the ML scheme becomes much more significant when the precipitation data at the finer resolution are noisier. Although the MO schemes perform slightly worse in 4 scenarios (out of 12 scenarios) than the ML scheme at the coarser resolution, the fused precipitation data at the coarser resolution with the ML scale are already quite good as shown in the work of Wang et al. [Wang et al., 2011]. Thus, the slightly under-performance by the MO schemes at the coarser resolution is not a cause for concern. Overall, the good performance by the MO schemes over the ML scheme is promising.

The three MO schemes perform differently on improving the spatial pattern of precipitation data at the finer resolution. For most of the scenarios, the mean, the median, the upper quartile and the lower quartile of the $\Delta Corr_7$ of the #3 MO scheme are clearly larger than corresponding ones of the #1 and the #2 MO schemes. #2 MO scheme performs slightly better than or the same as the #1 MO scheme. This implies again that the log-likelihood function (i.e., Equ. 4) included in the #2 MO scheme doesn't bring any significant gain to the fused precipitation data. That is, the effect of the likelihood function is indirectly represented by those of equations (5-8). However, the information entropy represented by equations 9 and 10 does bring in more information than that by equations 7 and 8 at a cost of doubling the computational time.

Results of $\Delta Corr_7$ of the ML scheme and the MO schemes for each scenario are also evaluated using statistical hypothesis tests. Based on the Q-Q plot (figures not shown), we find that none of the distributions of $\Delta Corr_7$ follow the normal distribution. Therefore, we use the Kolmogorov-Smirnov test to examine the differences of $\Delta Corr_7$ between the ML scheme and the MO schemes to check whether they are significantly different. Unlike the paired t-test, which only works well with normal distributions, the Kolmogorov-Smirnov test can be used for cases following any type of continuous distributions. The null hypothesis is that the differences are not significant and the alternative hypothesis is that the differences are significant. Results of the Kolmogorov-Smirnov test (at 1% significant level) show that the distribution differences of $\Delta Corr_7$ between the MO schemes and the ML scheme are significant for all of the 12 scenarios shown in Figure 5. These results confirm again the significantly better performances with the MO schemes than those with the ML scheme at the finer resolution. Based on our results, we can infer that the MO schemes are significantly superior to the ML scheme in deriving fused precipitation data at finer resolutions in terms of improving the spatial patterns of the precipitation. The #1 MO scheme is a better choice for limited computational resources and the #3 MO scheme is a better choice when computational resources are sufficient.

Figure 6 shows the box plots of $\Delta RMSE_s$ ($s = 5, 7$) for the 12 scenarios. Like Figure 5, each scenario has multiscale precipitation data fusion with the ML scheme and the three MO schemes. In Figure 6, if the MO schemes lead to larger values of $\Delta RMSE_s$, it indicates that statistically, the MO schemes perform better than the ML scheme. Otherwise, the MO schemes are statistically not as good as the ML scheme. In addition, if any of the MO scheme results in higher values of $\Delta RMSE_s$, it means that the MO scheme has a

632 better choice of the objective functions in terms of improving the magnitudes of fused
633 precipitation data.

634 In Figure 6, the differences of $\Delta RMSE_5$ between the ML scheme and the MO schemes
635 are relatively small for all of the 12 scenarios compared to the corresponding differences of
636 $\Delta RMSE_7$. The superiorities of the MO schemes or the ML schemes depend on the noise
637 levels at both scales. Specifically, the performance of the MO schemes is slightly better
638 than that of the ML scheme when $n_5 > n_7$, i.e. for the combinations of $n_5 = 2.0$ and
639 $n_7 = 1.0$, $n_5 = 3.0$ and $n_7 = 1.0$, and $n_5 = 3.0$ and $n_7 = 2.0$. This indicates that the MO
640 schemes are better choices than the ML scheme when fusing much noisier precipitation
641 data at a coarser resolution with less noisy data at a finer resolution. When $n_5 \leq n_7$,
642 i.e., when the precipitation data at the finer resolution is noisier than that at the coarser
643 resolution, the performances of the MO schemes are slightly worse than that of the ML
644 scheme. For example, the lower and the upper quartiles and the medians of $\Delta RMSE_5$ of
645 the MO schemes are smaller than those of $\Delta RMSE_5$ of the ML scheme for the scenarios
646 of $n_5=n_7=1.0$, 2.0 and 3.0, $n_5 = 1.0$ and $n_7 = 2.0$, $n_5 = 1.0$ and $n_7 = 4.0$, $n_5 = 2.0$ and
647 $n_7 = 3.0$, $n_5 = 2.0$ and $n_7 = 4.0$, and $n_5 = 3.0$ and $n_7 = 4.0$. But most of the differences
648 are very small or negligible. Since the fused precipitation data at the coarser resolution
649 with the ML scale are already quite good as shown in the work of Wang et al. [Wang
650 et al., 2011], the smaller values of $\Delta RMSE_5$ with the MO scheme than those with the
651 ML scheme are not a cause for concern. Among the three MO schemes, the #1 and #2
652 MO schemes perform very closely. This once again shows that the objective functions of
653 #1 MO scheme are sufficient enough and there is no need to add the likelihood function.

The #3 MO scheme is slightly better than the #1 and the #2 MO schemes for most of scenarios.

On the other hand, the MO schemes perform much better than the ML scheme on improving the magnitude of the fused precipitation data at the finer resolution. As shown in Figure 6, the lower and the upper quartiles, the means and medians of the $\Delta RMSE_7$ of the MO schemes are clearly higher than the corresponding counterparts of the ML scheme for all of the 12 scenarios. The differences between $\Delta RMSE_7$ of the MO schemes and $\Delta RMSE_7$ of the ML scheme are also examined using the Kolmogorov-Smirnov test (at 1% significant level) similar to the correlation cases shown in Figure 5. Again the test results indicate that all of the differences are statistically significant. This implies that the MO schemes are significantly superior to the ML scheme in terms of improving the magnitudes of the fused precipitation at the finer spatial resolution using the MKS algorithm. Among the three MO schemes, the #1 and the #2 MO schemes behave similarly while the #3 MO scheme also obviously better than the #1 and #2 MO schemes because of its higher values of the lower and the upper quartiles, the mean and the median.

Figure 7 shows a precipitation event before (i.e., X_5^- and X_7^-) and after (i.e., X_5^+ and X_7^+) the precipitation data fusion using the MKS algorithm with the #3 MO scheme. In the figure, the synthetically generated noisy precipitation fields (X_5^- and X_7^-) are for the precipitation event at 09Z 09/22/2003 with $n_5 = 2.0$ and $n_7 = 2.0$. The true precipitation image of this event at scale 7 is shown in Figure 2. Comparing the precipitation field in Figure 1 with X_5^- and X_7^- in Figure 7, one can see clearly that the spatial pattern of the true precipitation field has been heavily contaminated in the synthetic precipitation fields at both scales 5 and 7. After the data fusion using the MKS algorithm with the #3 MO

scheme, the original spatial pattern has been mostly restored at both scales. However, the fused precipitation data at scale 7 have lost some details at scale 7. This is a common drawback of improving precipitation data of finer resolution with precipitation data of coarser resolution. It also partially comes from one of the constraints of the MO schemes, i.e. the one shown in equation 6. A relaxation of equation 6 may relieve the losing of details at the finer resolution.

5. Conclusions

This paper presents a general multi-objective (MO) parameter estimation scheme for the Multiscale Kalman Smoother (MKS) algorithm used in precipitation data fusion. Three approaches have been introduced with it to avoid over-smoothing of precipitation data. Formulations for this MO parameter estimation scheme are established based on the understanding of the objectives for the multiscale precipitation data fusion. The objective functions of each specific MO scheme have clear physical meanings that are related to precipitation data. This helps to make fused precipitation data to meet the expectations at multiscale scales. A Monte Carlo experiments have been conducted to reveal the limitations of the maximum likelihood (ML) scheme for the multiscale precipitation data fusion. The Monte Carlo experiment study justifies the rationale to develop the multi-objective parameter (MO) estimation scheme, which significantly enhances the performance of the Multiscale Kalman Smoother at the finer resolutions. The proposed multi-objective parameter estimation scheme has been extensively evaluated against the conventional maximum likelihood scheme (ML) over 2246 precipitation events in 2003 with regard to improving the spatial patterns and the magnitudes of the precipitation data based on the results of 12 scenario experiments.

Studies in this paper can be summarized through two aspects. First, the limitations of the maximum likelihood scheme for estimating the parameters of the Multiscale Kalman Smoother algorithm have been revealed for applications in the real world precipitation data fusion. This scheme does not work well at finer resolutions even though it is effective at coarser resolutions. At the finer resolution, it is possible that only limited improvements can be achieved on the fused precipitation data in their spatial patterns and magnitudes using the Kalman Smoother algorithm and the maximum likelihood scheme. The reasons are due to the combinations that (1) the assumptions made in the ML scheme are not always met, and (2) local optimal instead of global optimal are obtained. In order to improve the performance at the finer resolutions, we developed a multi-objective (MO) parameter estimation scheme for the Multiscale Kalman Smoother algorithm. In the scheme, we formulated two core objective functions (equation 5 and 6) to simultaneously improve the spatial patterns and the magnitudes of the fused precipitation data at multiple scales. Three different approaches have been investigated with the MO scheme to reduce over-smoothing of precipitation details at the finer resolution.

Comparisons between our new MO schemes and the ML scheme over a large number of precipitation events show that the proposed MO schemes have significantly better performances on improving the qualities of the fused precipitation data at the finer spatial resolution. The superiority of the MO schemes is even higher than that of the ML scheme when the precipitation data at the finer spatial resolutions are much noisier than the precipitation data at the coarser spatial resolutions. At the coarser spatial resolution, if the precipitation data are noisier than the precipitation data at the finer resolution, the new MO schemes also perform better than or comparable to that of the ML scheme on

improving the spatial patterns and the magnitudes of precipitation data. Among the three approaches related to the MO schemes, the #1 and the #2 approaches work very similarly at both spatial scales. This means that the likelihood function (i.e., equation 4) could be mostly represented by equations 7 - 8. The #3 approach results in better performance of the MKS algorithm than those of the #1 and #2 approaches. This means that the objective functions of the information entropy could bring in more useful information to fused precipitation data than the two objective functions of maximization (i.e., equation 7 and 8). The #3 MO scheme is a better choice than the #1 MO scheme only if the computational resources is not limited. Otherwise, the #1 MO scheme is a good choice.

Second, our numerical results have shown that the MO scheme can effectively represent the main features characterized by the ML scheme for the fused precipitation data at finer resolution. In the results of section 4.2, the #2 MO scheme does not show advantages to the #1 MO scheme for most cases. The advantages are negligible if any. The #3 MO scheme over-performs the #2 MO scheme generally. This implies that the two objective functions of the information entropy may represent even more information than the log-likelihood function. Thus, results obtained from the #3 MO scheme can be considered to have similar or even more strengths than those with the ML scheme.

In summary, the multi-objective (MO) parameter estimation scheme, referred here as a general term to include the three different individual approaches, i.e., the #1, #2, and #3 MO schemes, is effective for the Multiscale Kalman Smoother algorithm in fusing precipitation data, especially for deriving precipitation data products at finer spatial resolutions where large improvements are achieved compared to the ML scheme. On the other hand, the MO scheme takes longer computational time due to its multi-objective optimization

process. If the fused precipitation data products are desired at coarser spatial resolutions, the maximum likelihood (ML) scheme is recommended. But if the fused precipitation data are desired at finer spatial resolutions, the multi-objective (MO) parameter estimation scheme is highly recommended due to its much better performances at the finer spatial resolutions while its performances at the coarse resolutions are also very good. The concepts and ideas of our MO schemes in combining with the MKS algorithm are general, and thus can also be applied, in combination, to other approaches as well.

Acknowledgments. We thank Dr. Server Levent Yilmaz for his help in providing computing assistance of using the TeraGrid resources. This work was partially supported by the NASA grants of NNA07CN83A and NNX12AQ25G to the University of Pittsburgh.

References

- Bocchiola, D. (2007), Use of scale recursive estimation for assimilation of precipitation data from trmm (pr and tmi) and nexrad, *Advances In Water Resources*, 30(11), 2354–2372, doi:DOI 10.1016/j.advwatres.2007.05.012.
- Chou, K., A. Willsky, and R. Nikoukhah (1994), Multiscale systems, kalman filters, and riccati-equations, *Ieee Transactions On Automatic Control*, 39(3), 479–492.
- Chou, K. C. (1996), Maximum-likelihood estimation of multiscale stochastic model parameters, in *Proc. IEEE-SP International Symposium on Time-Frequency and Time-Scale Analysis*, pp. 17–20.
- Chou, K. C., and A. S. Willsky (1991), Modeling and estimation of multiscale processes, in *Signals, Systems and Computers, 1991. 1991 Conference Record of the Twenty-Fifth Asilomar Conference on*, pp. 778–784 vol.2.

- 766 Cosgrove, B. A., et al. (2003), Real-time and retrospective forcing in the north american
767 land data assimilation system (nldas) project, *J. Geophys. Res.*, *108*(D22).
- 768 Digalakis, V., J. R. Rohlicek, and M. Ostendorf (1993), Ml estimation of a stochastic
769 linear system with the em algorithm and its application to speech recognition, *Ieee*
770 *Transactions On Speech and Audio Processing*, *1*(4), 431–442.
- 771 Gill, M. K., Y. H. Kaheil, A. Khalil, M. McKee, and L. Bastidas (2006), Multiobjective
772 particle swarm optimization for parameter estimation in hydrology, *Water Resources*
773 *Research*, *42*(7), W07,417, doi:DOI 10.1029/2005WR004528.
- 774 Gorenburg, I., D. McLaughlin, and D. Entekhabi (2001), Scale-recursive assimilation of
775 precipitation data, *Advances In Water Resources*, *24*(9-10), 941–953.
- 776 Gupta, R., V. Venugopal, and E. Foufoula-Georgiou (2006), A methodology for merg-
777 ing multisensor precipitation estimates based on expectation-maximization and scale-
778 recursive estimation, *Journal of Geophysical Research-Atmospheres*, *111*(D2), D02,102,
779 doi:DOI 10.1029/2004JD005568.
- 780 Hu, X., and R. Eberhart (2002), Multiobjective optimization using dynamic neighborhood
781 particle swarm optimization, in *Evolutionary Computation, 2002. CEC '02. Proceedings*
782 *of the 2002 Congress on*, vol. 2, pp. 1677 –1681, doi:10.1109/CEC.2002.1004494.
- 783 Hu, X., R. C. Eberhart, and Y. Shi (2003), Particle swarm with extended memory for mul-
784 tiobjective optimization, in *Swarm Intelligence Symposium, 2003. SIS '03. Proceedings*
785 *of the 2003 IEEE*, pp. 193–197.
- 786 Huang, H., N. Cressie, and J. Gabrosek (2002), Fast, resolution-consistent spatial pre-
787 diction of global processes from satellite data, *Journal of Computational and Graphical*
788 *Statistics*, *11*(1), 63–88.

- Jayakrishnan, R., R. Srinivasan, and J. G. Arnold (2004), Comparison of raingage and
wsr-88d stage iii precipitation data over the texas-gulf basin, *Journal of Hydrology*,
292(1-4), 135–152.
- Kannan, A., M. Ostendorf, W. Karl, D. Castanon, and R. Fish (2000), Ml parameter
estimation of a multiscale stochastic process using the em algorithm, *Ieee Transactions
On Signal Processing*, 48(6), 1836–1840.
- Kennedy, J., and R. Eberhart (1995), Particle swarm optimization, in *Neural Networks,
1995. Proceedings., IEEE International Conference on*, vol. 4, pp. 1942–1948 vol.4.
- Kumar, P. (1999), A multiple scale state-space model for characterizing subgrid scale
variability of near-surface soil moisture, *Ieee Transactions On Geoscience and Remote
Sensing*, 37(1), 182–197.
- Ly, S., C. Charles, and A. Degré (2011), Geostatistical interpolation of daily rainfall
at catchment scale: the use of several variogram models in the ourthe and ambleve
catchments, belgium, *Hydrology and Earth System Sciences*, 15(7), 2259–2274, doi:
10.5194/hess-15-2259-2011.
- Nan, Z. T., S. G. Wang, X. Liang, T. E. Adams, W. Teng, and Y. Liang (2010), Analysis of
spatial similarities between nexrad and nldas precipitation data products, *Ieee Journal
of Selected Topics in Applied Earth Observations and Remote Sensing*, 3(3), 371–385.
- Parada, L., and X. Liang (2004), Optimal multiscale kalman filter for assimilation of
near-surface soil moisture into land surface models, *Journal of Geophysical Research-
Atmospheres*, 109(D24), D24,109, doi:DOI 10.1029/2004JD004745.
- Parada, L. M., and X. Liang (2008), Impacts of spatial resolutions and data quality on soil
moisture data assimilation, *Journal of Geophysical Research-Atmospheres*, 113(D10),

D10,101, doi:DOI 10.1029/2007JD009037.

Simone, G., F. C. Morabito, and A. Farina (), Radar image fusion by multiscale kalman filtering, in *Proc. Third International Conference on Information Fusion FUSION 2000*, vol. 2, edited by F. C. Morabito, pp. WED3/10–WED3/17 vol.2.

Slatton, K., M. Crawford, and B. Evans (2001), Fusing interferometric radar and laser altimeter data to estimate surface topography and vegetation heights, *Ieee Transactions On Geoscience and Remote Sensing*, 39(11), 2470–2482.

Slatton, K. C., M. Crawford, and L. Teng (2002), Multiscale fusion of insar data for improved topographic mapping, in *Proc. IEEE International Geoscience and Remote Sensing Symposium IGARSS '02*, vol. 1, edited by M. Crawford, pp. 69–71 vol.1.

Smith, J. A., and W. F. Krajewski (1991), Estimation of the mean field bias of radar rainfall estimates, *Journal of Applied Meteorology*, 30(4), 397–412.

Sorooshian, S., K. L. Hsu, X. Gao, H. V. Gupta, B. Imam, and D. Braithwaite (2000), Evaluation of persiann system satellite-based estimates of tropical rainfall, *Bulletin of the American Meteorological Society*, 81(9), 2035–2046.

Tian, Y. D., and C. D. Peters-Lidard (2010), A global map of uncertainties in satellite-based precipitation measurements, *Geophysical Research Letters*, 37, –.

Tustison, B., E. Foufoula-Georgiou, and D. Harris (2002), Scale-recursive estimation for multisensor quantitative precipitation forecast verification: A preliminary assessment, *Journal of Geophysical Research-Atmospheres*, 108(D8), 8377, doi:DOI 10.1029/2001JD001073.

Ushio, T., et al. (2009), A kalman filter approach to the global satellite mapping of precipitation (gsmmap) from combined passive microwave and infrared radiometric data,

835 *Journal of the Meteorological Society of Japan*, 87, 137–151.

836 Van de Vyver, H., and E. Roulin (2009), Scale-recursive estimation for merging precip-
837 itation data from radar and microwave cross-track scanners, *Journal of Geophysical*
838 *Research-Atmospheres*, 114, D08,104, doi:DOI 10.1029/2008JD010709.

839 Voisin, N., A. W. Wood, and D. P. Lettenmaier (2008), Evaluation of precipitation prod-
840 ucts for global hydrological prediction, *Journal of Hydrometeorology*, 9(3), 388–407.

841 Wang, S. (2011), Assessments of multiscale precipitation data fusion and soil moisture
842 data assimilation and their roles in hydrological forecasts, Ph.D. thesis, University of
843 Pittsburgh.

844 Wang, S., X. Liang, and Z. Nan (2011), How much improvement can precipitation data
845 fusion achieve with a multiscale kalman smoother-based framework?, *Water Resources*
846 *Research*, 47, W00H12, doi:DOI 10.1029/2010WR009953.

847 Wang, X., H. Xie, H. Sharif, and J. Zeitler (2008), Validating nexrad mpe and
848 stage iii precipitation products for uniform rainfall on the upper guadalupe river
849 basin of the texas hill country, *Journal of Hydrology*, 348(1-2), 73–86, doi:DOI
850 10.1016/j.jhydrol.2007.09.057.

851 Willsky, A. (2002), Multiresolution markov models for signal and image processing, *Pro-*
852 *ceedings of the Ieee*, 90(8), 1396–1458, doi:DOI 10.1109/JPROC.2002.800717.

Figure 1. An example of multiscale tree: a two-dimensional multiscale tree with three spatial scales. For node t at scale 1, $t\bar{\gamma}$ represents its parent node and $t\alpha_n$ ($n = 1, 2, 3, 4$) represents its child nodes. Without a parent, the node at scale 0 (i.e., the coarsest resolution) is called a root node; without any child nodes, the nodes at scale 2 (i.e., the finest resolution) are called leaf node.

Figure 2. Map of experiment domain. Gray mesh represents 32×32 grids at $1/8^\circ$ resolution. This map illustrates the NEXRAD MPE precipitation data at 09Z 09/22/2003, which are used as the true data in the Monte Carlo experiment in section 4.2. The unit of precipitation data is mm/hr.

Figure 3. Boxplots of the correlation and RMSE between the true and the synthetic precipitation data in 2003. The horizontal axes of subplots $Corr_5^-$ and $RMSE_5^-$ are the noise levels at scale 5, i.e. x_5 ; the horizontal axes of subplots $Corr_7^-$ and $RMSE_7^-$ are noise level at scale 7, i.e. x_7 . For each box, the bottom and the top represent the lower (25^{th}) quartile and the upper (75^{th}) quartile, the lower and the upper whiskers represent 1.5 IQR (interquartile range) of the lower quartile and 1.5 IQR of the upper quartile, and the black dot represents the mean of $Corr$ or $RMSE$.

Figure 4. Scatter plots of log-likelihood and $Corr_5^+$, log-likelihood and $Corr_7^+$, log-likelihood and $RMSE_5^+$, and log-likelihood and $RMSE_7^+$. The horizontal axes of all subplots are log-likelihood.

Figure 5. Boxplots of $\Delta Corr_5$ and $\Delta Corr_7$ computed after the multiscale precipitation data fusion using the MKS algorithm with the ML scheme (in black color) and the MO schemes (in red, green, and blue colors) for the 12 scenarios. In the labels of the horizontal axes of all subplots, C denotes $\Delta Corr$ and the supper scripts 0, 1, 2, and 3 denotes the ML scheme and the MO schemes. The title of each subplot describes the combination of noise levels at scale 5 and scale 7 of the scenario. Descriptions of symbols are the same as those in Figure 3.

Figure 6. Boxplots of $\Delta RMSE_5$ and $\Delta RMSE_7$ computed after the multiscale precipitation data fusion using the MKS algorithm with the ML scheme and the MO schemes for the 12 scenarios. The descriptions of labels and symbols are the same as those in Figure 5.

Figure 7. Example of multiscale precipitation data fusion using the MKS algorithm with the MO scheme ($n_5 = 2.0$ and $n_7 = 2.0$) at 09Z 09/22/2003. X_5^- and X_5^+ denote synthetic precipitation data and fused precipitation data at $1/8^\circ$ resolution (scale 5). X_7^- and X_7^+ denote synthetic precipitation data and fused precipitation data at $1/32^\circ$ resolution (scale 7).

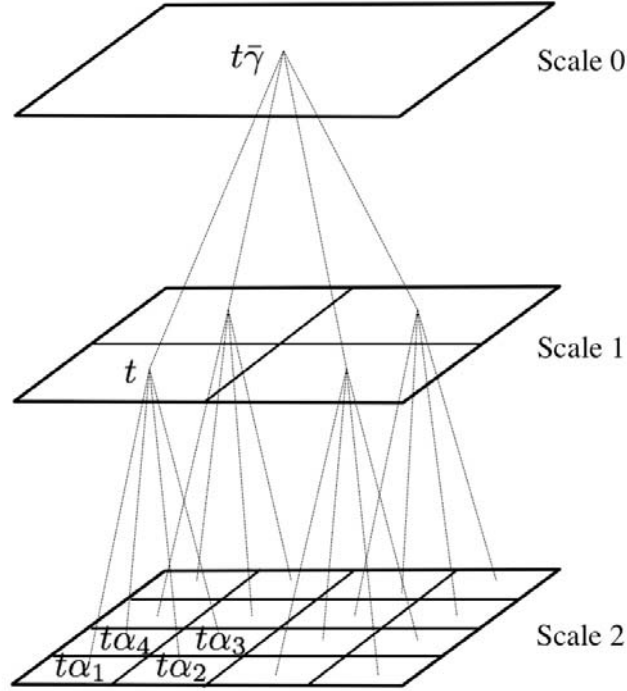


Figure 1: An example of multiscale tree: a two-dimensional multiscale tree with three spatial scales. For node t at scale 1, $t\bar{\gamma}$ represents its parent node and $t\alpha_n$ ($n = 1, 2, 3, 4$) represents its child nodes. Without a parent, the node at scale 0 (i.e., the coarsest resolution) is called a root node; without any child nodes, the nodes at scale 2 (i.e., the finest resolution) are called leaf node.

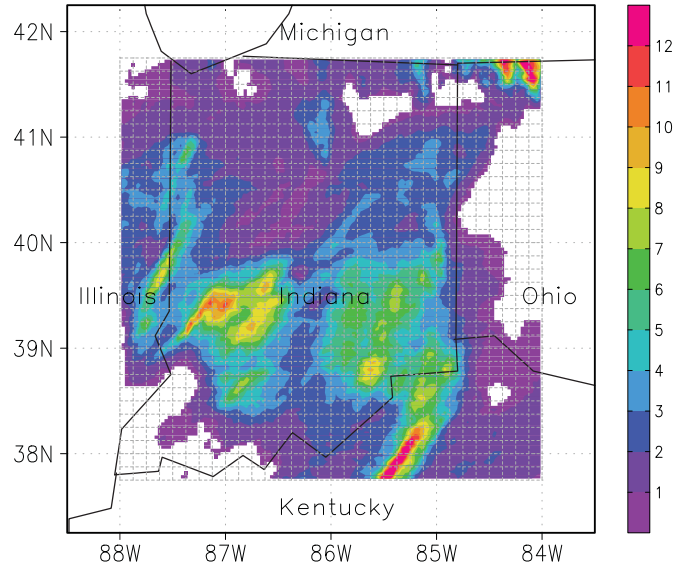


Figure 2: Map of experiment domain. Gray mesh represents 32×32 grids at $1/8^\circ$ resolution. This map illustrates the NEXRAD MPE precipitation data at 09Z 09/22/2003, which are used as the true data in the Monte Carlo experiment in section 4.2. The unit of precipitation data is mm/hr.

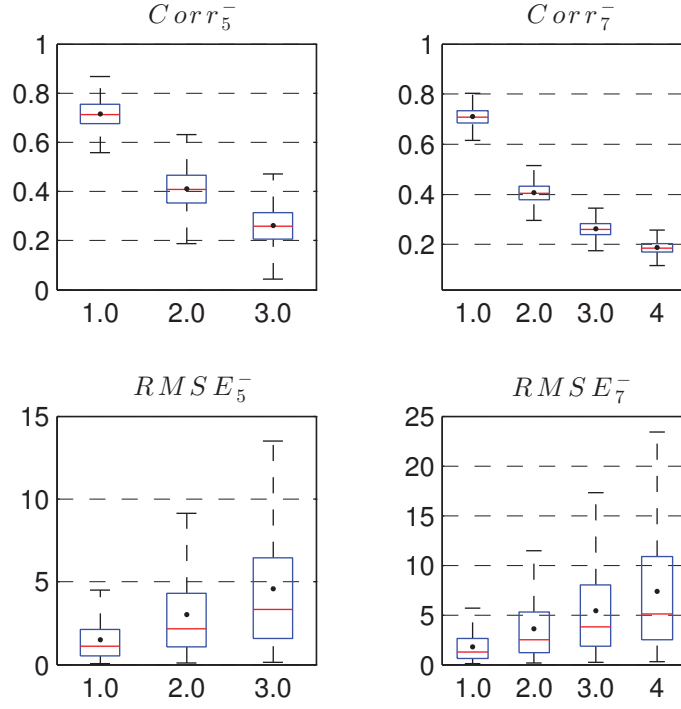


Figure 3: Boxplots of the correlation and RMSE between the true and the synthetic precipitation data in 2003. The horizontal axes of subplots $Corr_5^-$ and $RMSE_5^-$ are the noise levels at scale 5, i.e. x_5 ; the horizontal axes of subplots $Corr_7^-$ and $RMSE_7^-$ are noise level at scale 7, i.e. x_7 . For each box, the bottom and the top represent the lower (25th) quartile and the upper (75th) quartile, the lower and the upper whiskers represent 1.5 IQR (interquartile range) of the lower quartile and 1.5 IQR of the upper quartile, and the black dot represents the mean of $Corr$ or $RMSE$.

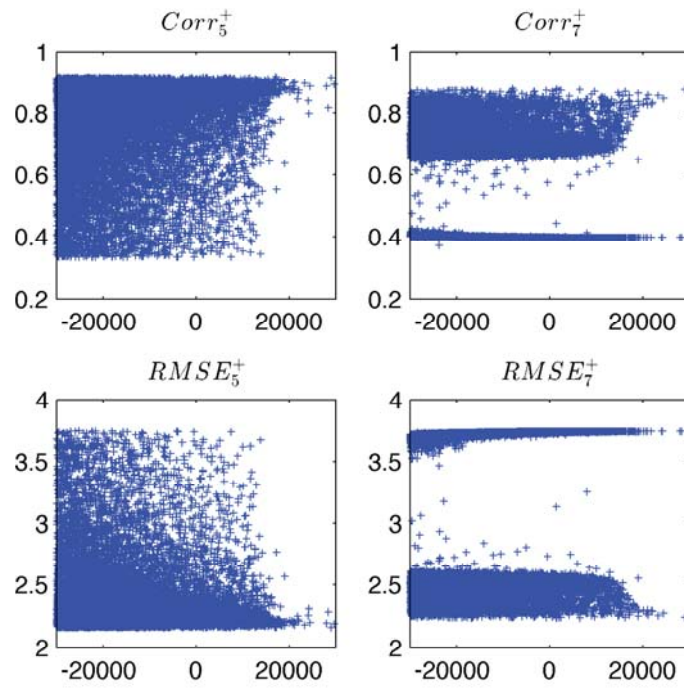


Figure 4: Scatter plots of log-likelihood and $Corr_5^+$, log-likelihood and $Corr_7^+$, log-likelihood and $RMSE_5^+$, and log-likelihood and $RMSE_7^+$. The horizontal axes of all subplots are log-likelihood.

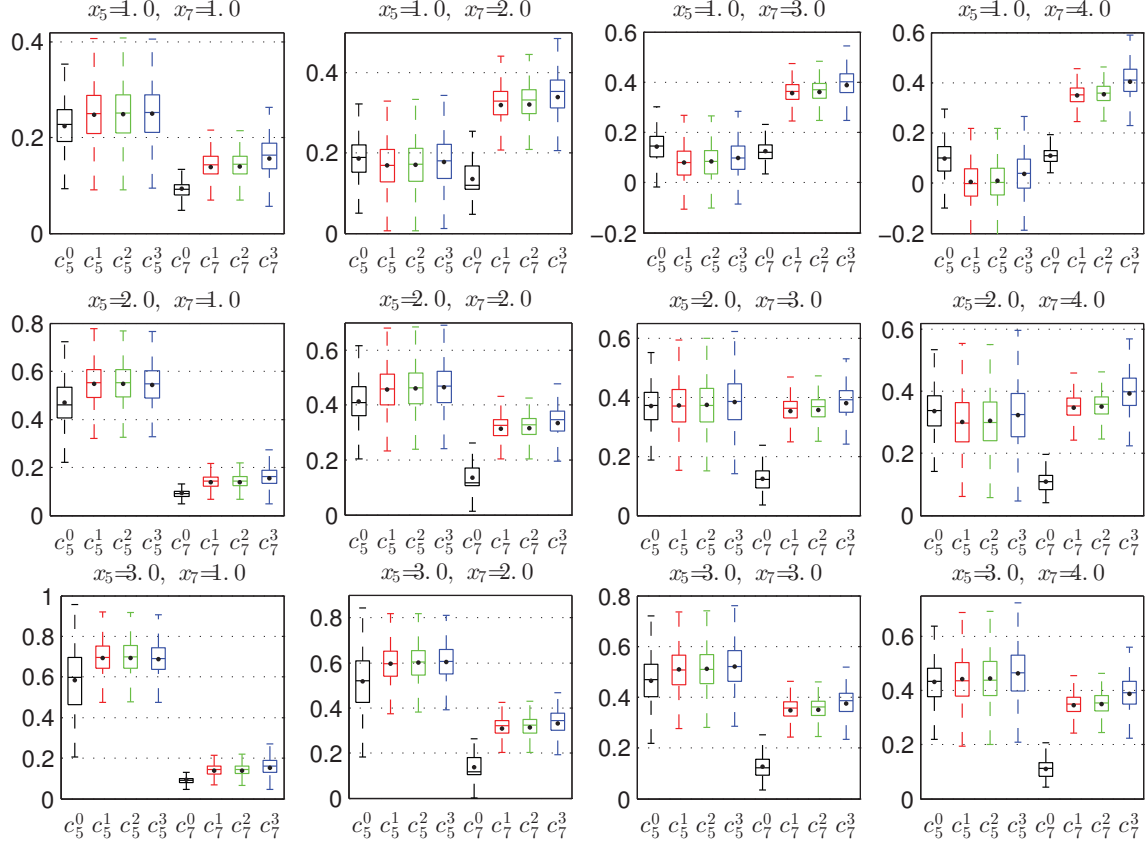


Figure 5: Boxplots of $\Delta Corr_5$ and $\Delta Corr_7$ computed after the multiscale precipitation data fusion using the MKS algorithm with the ML scheme (in black color) and the MO schemes (in red, green, and blue colors) for the 12 scenarios. In the labels of the horizontal axes of all subplots, C denotes $\Delta Corr$ and the supper scripts 0, 1, 2, and 3 denotes the ML scheme and the MO schemes. The title of each subplot describes the combination of noise levels at scale 5 and scale 7 of the scenario. Descriptions of symbols are the same as those in Figure 3.

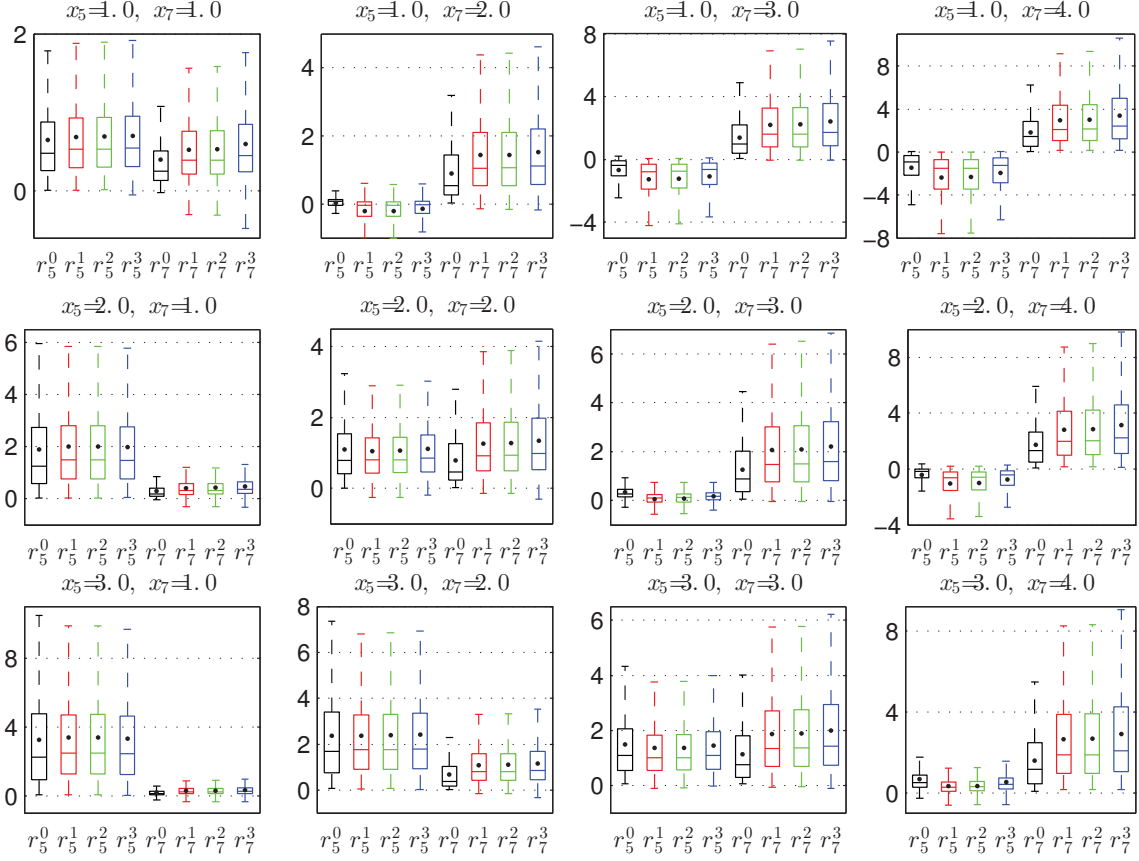


Figure 6: Boxplots of $\Delta RMSE_5$ and $\Delta RMSE_7$ computed after the multiscale precipitation data fusion using the MKS algorithm with the ML scheme and the MO schemes for the 12 scenarios. The descriptions of labels and symbols are the same as those in Figure 5.

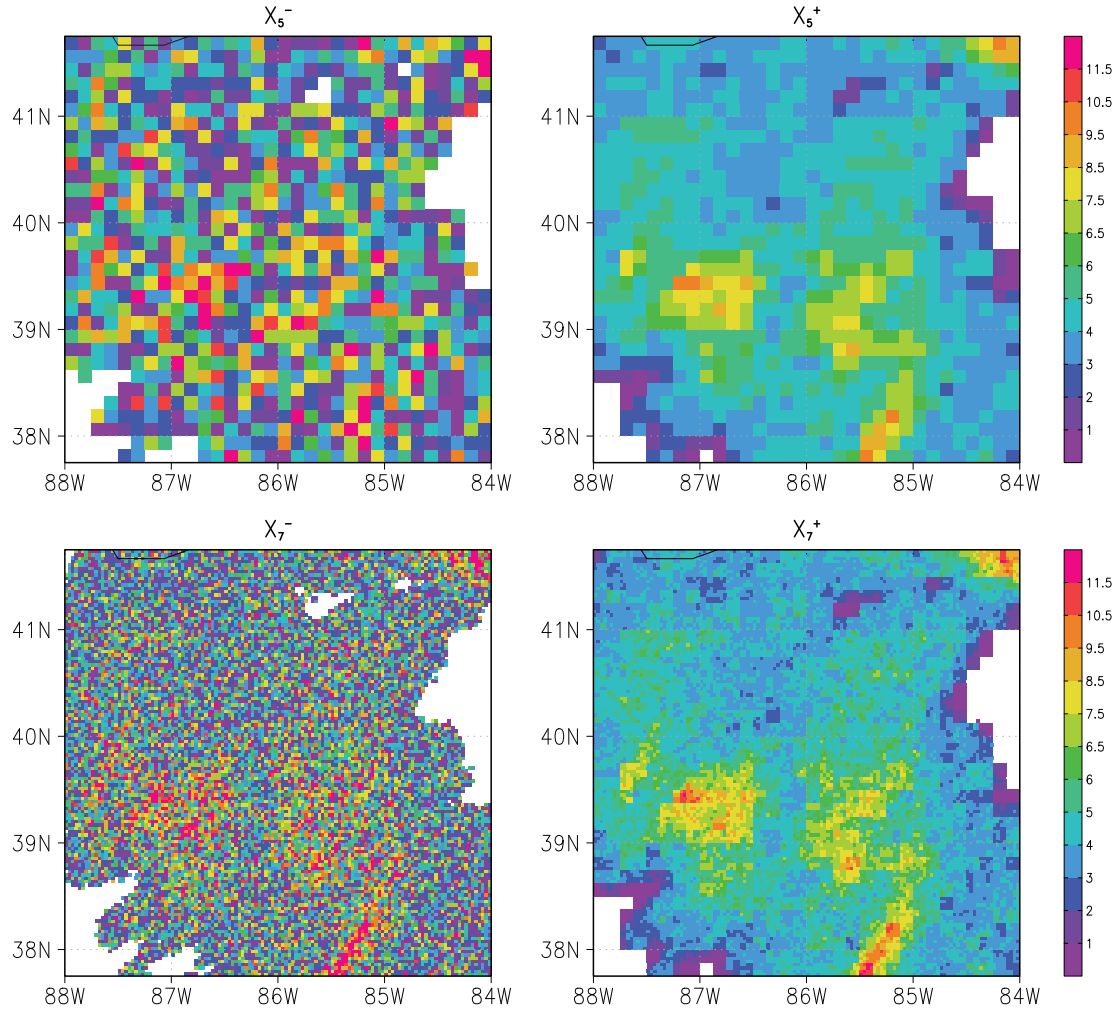


Figure 7: Example of multiscale precipitation data fusion using the MKS algorithm with the MO scheme ($n_5 = 2.0$ and $n_7 = 2.0$) at 09Z 09/22/2003. X_5^- and X_5^+ denote synthetic precipitation data and fused precipitation data at $1/8^\circ$ resolution (scale 5). X_7^- and X_7^+ denote synthetic precipitation data and fused precipitation data at $1/32^\circ$ resolution (scale 7).